2025年臺灣國際科學展覽會
優勝作品專輯

作品編號　030030

參展科別　化學

作品名稱　Synthesis of fluconazole analogues with focusing on resistant strains Candida

得獎獎項　二等獎

就讀學校　Moscow South-Eastern School named after V.I. Chuikov

指導教師　Ksenia Salnikova

作者姓名　Adelina Vakhitova

作者照片

MSES Moscow South-Eastern School named after V.I. Chuikov

A. N. Belozersky Research Institute of Physico-Chemical Biology MSU

Synthesis of fluconazole analogues with focusing on resistant strains *Candida*

Adelina Vakhitova
Moscow South-Eastern School named after V.I. Chuikov, 10th grade

Supervisors:
Alexander Yu. Rudenko
A.N. Belozersky Research Institute of Physico-Chemical Biology MSU

Ratislav M. Ozhiganov
HCC RAS, D. I. Mendeleev Russian University of Chemical Technology

2024

List of abbreviations:

t-Bu	tert-butyl $(CH_3)_3C$-
DIPEA	diisopropylethylamine
Et	ethyl C_2H_5-
HRMS	high resolution mass spectrometry
Me	methyl CH_3-
Ph	phenyl C_6H_5-
TLC	thin-layer chromatography
UV	ultraviolet
NMR	nuclear magnetic resonance spectroscopy

Abstract

Fungal infections, particularly those caused by resistant strains like *Candida auris* and *Candida glabrata*, pose a significant threat to global health. The widespread use of azole antifungals, such as fluconazole, has driven the emergence of multidrug-resistant strains, undermining the efficacy of existing treatments. These challenges necessitate the development of novel antifungal agents with enhanced activity and reduced resistance profiles.

To address resistance mechanisms, we designed and synthesized hybrid molecules combining triazole and thiazolidine-2,4-dione (TZD) pharmacophores. This strategy leverages dual mechanisms of action: inhibiting fungal CYP51, a key enzyme in ergosterol biosynthesis, and disrupting fungal cell wall integrity. The structural versatility of hybrid molecules allows for targeted modifications to enhance antifungal potency, binding specificity, and pharmacokinetics.

Using a stepwise synthetic approach, triazole-containing piperazine derivatives were first prepared and coupled with TZD-based carboxylic acids via optimized condensation reactions. The structures of the synthesized compounds were confirmed through advanced spectroscopic methods, including 1D/2D NMR and high-resolution mass spectrometry. The antifungal activity of these hybrids was evaluated in vitro against clinical and reference strains of *Candida spp.* and *Aspergillus fumigatus*. Among the synthesized compounds, 6a demonstrated notable activity against *Candida parapsilosis* (MIC 0.06 µg/mL), comparable to voriconazole. Compound 4b exhibited moderate activity against *C. parapsilosis* (MIC 1–2 µg/mL) and *A. fumigatus* (MIC 8 µg/mL). However, most compounds showed limited efficacy against highly resistant strains such as *C. albicans 8R* and *C. krusei*.

This study highlights the potential of hybrid triazole-TZD molecules in overcoming resistance and improving antifungal efficacy. While promising, further optimization is required to broaden the spectrum of activity and enhance efficacy against multidrug-resistant pathogens. These findings contribute to the growing field of antifungal drug development, emphasizing hybrid approaches as a viable solution for combating fungal resistance.

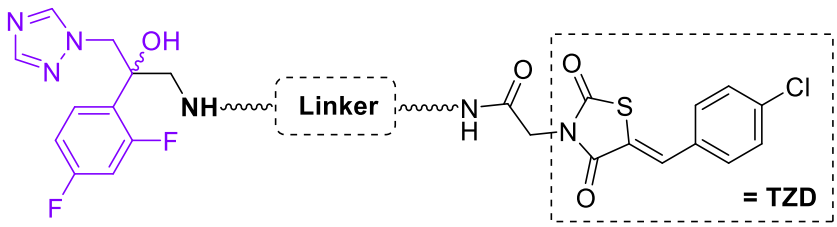

1. Introduction

Fungal infections, particularly those affecting internal organs, have become a significant global health concern in recent years. The World Health Organization (WHO) highlighted this crisis in October 2022, drawing attention to the insufficiency of current antifungal therapies and the rapid emergence of highly resistant fungal strains, such as *Candida auris*. The increased frequency of detection of naturally resistant strain, such as *Candida non-albicans* and *Candida auris*, has heightened the urgency of the issue. For instance, the proportion of fluconazole-resistant *Candida non-albicans* has risen from 0.3-0.5% to 45-50% in recent changes. This resistance poses a critical challenge to healthcare systems, as it undermines the efficacy of existing treatments and increases the risk of mortality associated with invasive fungal diseases.

Among the most concerning examples are the resistance patterns observed in *Candida glabrata* and *Candida auris*, alongside the rise of azole-resistant filamentous fungi, including *Aspergillus spp.* Furthermore, rarer mold fungi like *Mucor*, *Rhizopus*, and *Fusarium* continue to evade effective and reliable therapeutic options. These developments emphasize the urgent need for novel antifungal agents that can address resistance mechanisms and expand the spectrum of activity.

In this regard, there is a high demand for the development of drugs with new chemical structures and mechanisms of action that differ from known agents, in order to overcome the barrier of resistance. The coronavirus pandemic has revealed a significant problem related to human infections caused by pathogenic fungi. An international research group has found that up to 25% of deaths after coronavirus infection are associated with fungi. [J. Fungi 2020, 6, 91; doi:10.3390/jof6020091].

Limitations of Current Antifungal Therapies

The development of antifungal drugs is a complex and protracted process, hindered by the structural similarity between fungal and human cells. This similarity often results in off-target toxicity, limiting the therapeutic window of many antifungal agents. Azoles, such as fluconazole, voriconazole, and ravuconazole (Fig. 1), remain the most widely used class of antifungal drugs.

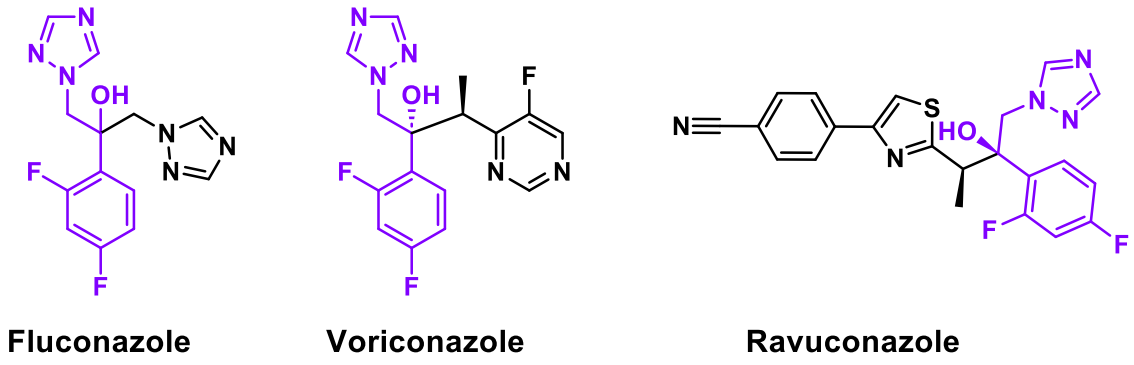

Figure 1. Azole class drugs used nowadays.

Azoles remain the main class of drugs for the treatment of fungal infections. They act by inhibiting lanosterol-14α-demethylase (CYP51), an enzyme that plays a key role in the biosynthesis of ergosterol, an important component of the fungal cell membrane. This leads to disruption of membrane integrity, increased membrane permeability, and cell death. However, the widespread use of azoles has resulted in a significant increase in resistant fungal strains, which seriously limits the effectiveness of these drugs.

The resistance of fungi to azoles is due to several mechanisms that allow the pathogen to survive and develop in the presence of antifungal drugs. These include changes in the structure of the target enzyme (CYP51). Mutations in the genes encoding CYP51 alter its structure, reducing the affinity of azoles to the active center of the enzyme. For example, mutations Y132H and S405F in *Candida albicans* are associated with high resistance to fluconazole. In some species (*Candida glabrata* and *Candida auris*), natural variations of CYP51 are observed, which reduce the effectiveness of azoles.

Another mechanism of resistance is the increased activity of efflux pumps. Fungi enhance the expression of transport proteins (efflux pumps), such as Cdr1, Cdr2, and Mdr1, which expel azoles from the cell, lowering their intracellular concentrations. This is particularly characteristic of resistant strains of *Candida glabrata* and *Candida auris.*

Some fungi can utilize bypass pathways in biosynthesis to produce membrane components, compensating for the lack of ergosterol. Resistant strains have been found to accumulate toxic intermediates, such as 14-methyl sterols, which can partially perform the functions of ergosterol.

Additionally, increased resistance occurs due to biofilm formation. Biofilms formed by fungi such as *Candida albicans* exhibit heightened resistance to azoles. Cells within biofilms are protected

from drug action due to a complex extracellular matrix and reduced access of the drug to the cells.

Resistance to azoles, particularly fluconazole, is most commonly observed among the following fungal species:

Resistant strains of *Candida auris* cause outbreaks of severe infections in hospitals. Its resistance to fluconazole exceeds 90% in some regions. *Candida glabrata* shows high resistance to fluconazole and reduced sensitivity to echinocandins. *Aspergillus fumigatus* is known for cases of multi-resistance, including resistance to voriconazole caused by mutations in CYP51A.

As a result, resistant strains significantly complicate the treatment of fungal infections and reduce the effectiveness of standard therapy. Patients infected with resistant strains often require combination or alternative therapies that may be more toxic and expensive. Additionally, resistance to azoles is associated with high mortality rates, especially in invasive infections. There are multi-resistant strains; for example, *Candida auris* can be transmitted in hospital settings, causing outbreaks that are difficult to control.

Other classes, such as echinocandins and polyenes, have provided alternatives but with significant limitations. Echinocandins, which inhibit β-glucan synthesis in the fungal cell wall, are ineffective against certain fungi, such as Cryptococcus and many molds. Polyenes like amphotericin B, while broad-spectrum, are often associated with severe nephrotoxicity, restricting their use.

Hybrid Molecules: A Promising Approach

In the search for improved antifungal agents, hybrid molecules combining multiple pharmacophores have emerged as a promising strategy. These molecules integrate the beneficial properties of individual pharmacophores, targeting multiple pathways or enhancing binding specificity. Triazole derivatives, in particular, have shown promise due to their broad-spectrum antifungal activity, minimal toxicity to mammalian cells, and clinical efficacy. The modification of the triazole pharmacophore, either through direct substitution or via linkers, offers opportunities to overcome resistance and optimize pharmacokinetics. This multifaceted approach not only enhances antifungal potency but also reduces the likelihood of resistance development, as pathogens must overcome several mechanisms of action simultaneously .

Hybrid molecules of triazole and thiazolidine-2,4-dione (TZD, Fig. 2) represent a novel approach to antifungal therapy. Triazoles are a cornerstone of modern antifungal treatment due to their high specificity for fungal lanosterol 14α-demethylase (CYP51), broad-spectrum activity, and clinical effectiveness. Modifying the triazole pharmacophore by incorporating additional structural elements, such as TZD, enhances its therapeutic potential. The inclusion of TZD provides unique advantages, including disrupting fungal cell wall integrity and interacting with alternative enzymatic targets. These dual-action hybrids can overcome traditional resistance mechanisms, such as efflux pump-mediated drug removal and mutations in CYP51.

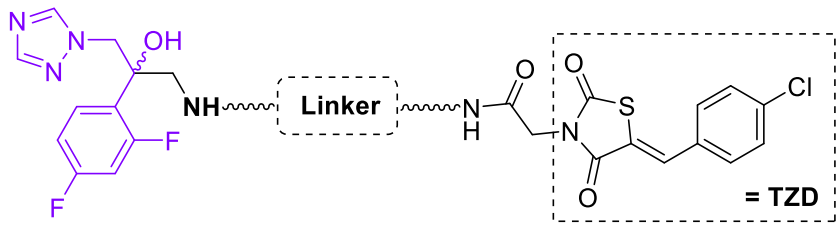

Figure 2. Hybrid molecules of triazole, thiazolidine-2,4-dione and linker

Hybridization allows the combination of complementary pharmacophores that increase affinity for the target. Additional structural components in hybrid molecules increase their specificity and binding strength with target proteins, such as CYP51, leading to improved antifungal activity and a reduction in the development of resistance. Furthermore, these modifications enable the optimization of the pharmacokinetics of the drugs. Structural modifications of hybrid compounds can enhance solubility, stability, and tissue penetration of the pharmaceuticals, thereby expanding their therapeutic applications.

For instance, recent studies have demonstrated that triazole-TZD hybrids effectively suppress the proliferation of fungi in strains resistant to conventional azoles. These compounds not only target CYP51 but also disrupt cell wall integrity, further amplifying their antifungal effects.

Recent studies have demonstrated the efficacy of such hybrids against resistant strains of *Candida auris*, *Candida non-albicans*, and *Aspergillus spp.*, with some compounds outperforming commercial azoles in in vitro and in vivo models.

Objectives of the Study

This study focuses on the synthesis and biological evaluation of new hybrid derivatives of triazole and TZD. The aim is to develop compounds with enhanced antifungal activity and improved

safety profiles, targeting multidrug-resistant fungi. Structural modifications are explored to optimize pharmacodynamic properties, with particular attention to linker design and substituent effects. By leveraging molecular modeling and microbiological assays, the study seeks to identify lead compounds that can overcome current therapeutic challenges and provide a foundation for future antifungal drug development.

The findings contribute to the growing body of research on antifungal hybrids, advancing the understanding of structure-activity relationships and offering innovative solutions to combat fungal resistance.

2. Results and Discussion

To start the synthesis, triazole-containing piperazine derivatives **3 a, b** were obtained by reaction of Boc-linker with either 2,4-difluorophenyl-substituted oxirane **1** (commercially available), which have been synthesized before. The reaction was carried out by reflux in ethanol with triethylamine. Then, the protecting group was removed by trifluoroacetic acid in dichloromethane (Scheme 1). The obtained compounds were characterized by NMR and mass spectrometry.

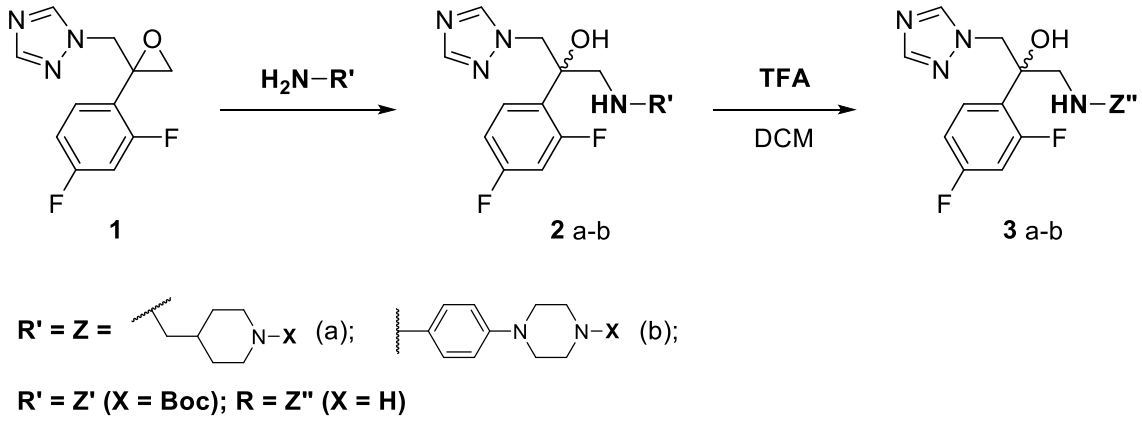

Scheme 1. Synthesis of piperazine-derived intermediates **3 a**-**b**.

Thiazolidine-substituted carboxylic acids (TZD, Scheme 2) were obtained from thiazolidine-2,4-dione by reproduction of the methods described in the literature. The carboxylic acids of TZD were transformed into acyl chlorides by action of thionyl chloride and immediately brought into reaction with N-substituted compounds 3a,b in CH_2Cl_2 at room temperature (Scheme 2). The use of other cross-linking reagents (TBTU and other) as a condensation agent resulted in a much lower yield. This way to the synthesis of the target compound 4a-b.

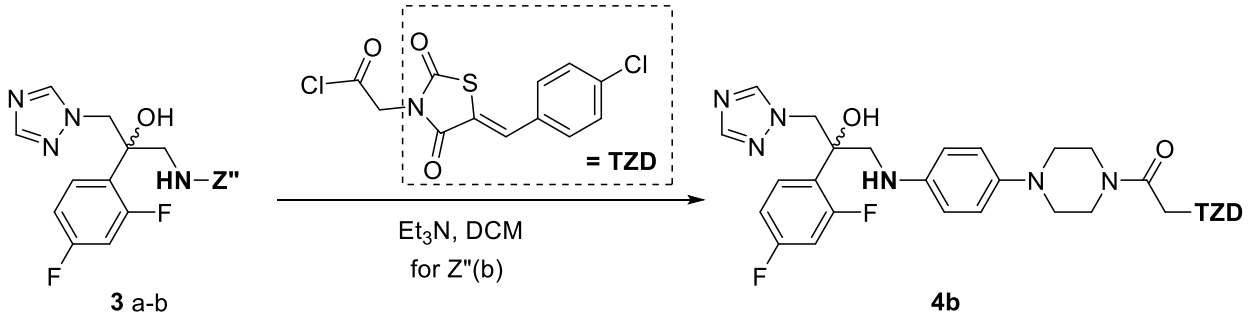

Scheme 2. Synthesis of hybrid piperazine amides 4b

The structures of key compound 4b were unambiguously confirmed by analysis of a series of 2D NMR experiments, including the homonuclear ^{1}H-^{1}H DQF-COSY and ROESY experiments, as well as the heteronuclear ^{13}C-^{1}H HSQC experiments and ^{13}C-^{1}H HMBC, performed at the natural abundance of the ^{13}C isotope. Analysis of these 2D spectra allowed us to completely assign the ^{1}H and ^{13}C signals of the compound 4b and to confirm their structure. Information on the assignment of the signals in the ^{1}H and ^{13}C spectra was further used in the interpretation of the 1D spectra of all other compounds studied.

Compounds containing various methyl **6a**, acetyl **9**, and p-fluorobenzoyl **10** groups in the linker chain have also been synthesized (Scheme 3). Literature data suggest that the introduction of substituents at this position increases the binding constant with CYP51.

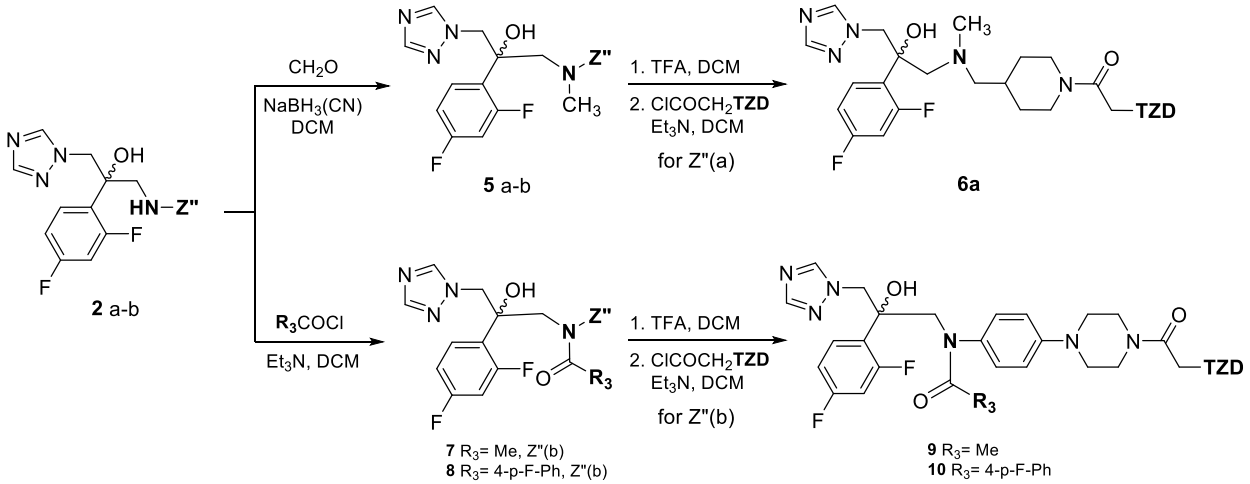

Scheme 3. Synthesis of hybrid piperazine amides 4b

A comparative study of the spectrum of the antifungal action of the new compounds was carried out in vitro by the method of using double micro-dilutions in broth, using standard strains and clinical isolates. For references, standard preparations of voriconazole were used, as well as the control strain of *Candida parapsilosis* (ATCC 22019). The minimal inhibitory concentration (MIC)

was taken as the lowest concentration of sample solutions at which at least 80% growth inhibition was observed. All experiments were repeated three times.

Table 1. In vitro antifungal action (MIC, μg/mL) of obtained compounds

Strains	MIC (ug/ml)						
	C.parapsilosis ATCC 22019		*C.albicans* 8R		*C. krusei* 432M		*A.fumigatus* ATCC 46645
	24h	48h	24h	48h	24h	48h	
voriconazole	0,06	0,06	≥32	≥32	0,5	1,0	0,25/0,5
2b	16	32	≥32	≥32	**4**	**8**	≥32
3b	32	≥32	≥32	≥32	≥32	≥32	≥32
4b	**1**	**2**	≥32	≥32	**8**	**8**	≥32
6a	**0,06**	**0,06**	≥32	≥32	**4**	**8**	≥32
7	32	≥32	≥32	≥32	≥32	≥32	≥32
8	32	≥32	≥32	≥32	≥32	≥32	≥32
9	32	≥32	≥32	≥32	≥32	≥32	≥32
10	32	≥32	≥32	≥32	≥32	≥32	≥32

Hybrid compounds exhibited varying activity depending on the strain (Table 1). Compound **6a** demonstrates a MIC of 0.06 μg/mL against *C. parapsilosis*, comparable to voriconazole, but efficacy against other strains remains low. Compound **4b** shows moderate activity against

C. parapsilosis (MIC 1–2 μg/mL) and A. fumigatus (MIC 8 μg/mL), but is also ineffective against *C. albicans* 8R and *C. krusei*. Most of the synthesized compounds (**2b, 3b, 7, 8, 9, 10**) exhibit MIC ≥ 32 μg/mL for all strains, indicating low or absent efficacy. This is particularly evident for *C. albicans* 8R and *C. krusei*, which demonstrate resistance even to the traditionally used antifungal agent voriconazole.

Hybrid compound **6a** shows potential comparable to voriconazole against *C. parapsilosis*; however, it loses effectiveness against other strains, necessitating further structural optimization. It is essential to evaluate the mechanisms of action of promising compounds to understand their specific effects and expand the series of derivatives based on compounds **4b** and **6a**.

3. Conclusions

The study confirmed the feasibility of synthesizing piperazine derivatives containing triazole and thiazolidine fragments using various linkers. The obtained compounds **2-10** were thoroughly characterized using NMR spectroscopy and mass spectrometry, which unequivocally confirmed their structures. Chemical modifications, such as the introduction of a methyl or benzoyl group in the linker chain, negatively affected the antifungal activity of the compounds. Several compounds demonstrated activity against *C. parapsilosis* (MIC 0.06 μg/mL), comparable to voriconazole, making it the most promising candidate for further research. Compounds **4b** and **6a** show potential for further modifications and optimization. Their structural features, particularly the influence of substituents in the linker, require more detailed analysis, including molecular docking simulations and testing against other clinically significant strains.

The study indicated that modifying the triazole pharmacophore and utilizing hybrid structures could be a promising approach for developing new antifungal agents. However, to achieve a broader spectrum of activity, additional optimization and testing of the obtained compounds are required.

4. Experimental section

Melting points were determined in open capillary tubes on a Mel-Temp® Instrument (Barnstead International, Dubuque, Iowa, USA) and are given uncorrected. High resolution ESI mass spectra were measured on a Waters Xevo G3 QTof (Waters, Framingham, USA) spectrometer. 1H NMR spectra were recorded on a Bruker AVANCE 600 spectrometer (600.13 MHz) at 25°C temperature. Chemical shifts for 1H NMR were reported as δ values and coupling constants were in Hertz (Hz). The following abbreviations were used for spin multiplicity: s = singlet, d = doublet, t = triplet, dd = double doublet, m = multiplet, bs = broad singlet. Chemical shifts were referenced to TMS as internal standard and reported in parts per million (ppm). All spectra were processed with MestReNova 14.2.2.

Thin-layer chromatography (TLC) analysis was conducted on silica gel plates (silica gel 60 Å, aluminum plates F254 from “Merck”). Chromatograms were visualized using a UV lamp (365 nm). Column chromatography was performed on silica gel 60 (230-400 mesh). The reagents used were obtained from commercial sources (“Acros”, “Sigma-Aldrich”) and used without further purification. All reactions were carried out using freshly distilled and dry solvents.

General method of synthesis 2a-b:

To a solution of compound 1 (1 mmol), ethanol (10 mL) was added amine (1.2 mmol) followed by the addition of triethylamine (3 mmol). The reaction was stirred at 80 °C for 6 h. After the reaction was completed (monitored by TLC, dichloromethane/methanol (20/1, v/v)), The solvent was evaporated under reduce pressure. The mixture was extracted with EtOAc 10 ml, the organic layer were washed with water 2×20ml, saturated sodium chloride solution, then dried over anhydrous Na_2SO_4, filtered, and concentrated in vacuum. The residue was purified by silica gel column chromatography (SiO_2, dichloromethane/methanol 25/1, v/v) to afford compound 2a-b.

Compound 2a

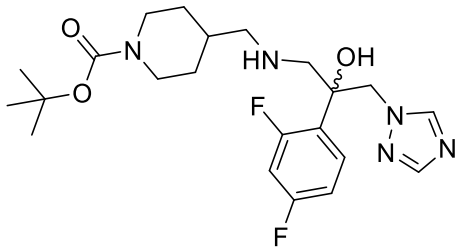

^{1}H NMR (600 MHz, $CDCl_3$) δ = 8.1 (s, 1H), 7.8 (s, 1H), 7.6 (q, *J*=6.5, 1H), 6.9 – 6.8 (m, 1H), 6.8 – 6.8 (m, 1H), 4.6 (d, *J*=14.3, 1H), 4.5 (d, *J*=14.3, 1H), 4.2 – 4.0 (m, 2H), 3.2 (d, *J*=12.6, 1H), 3.0 – 2.9 (m, 1H), 2.7 – 2.6 (m, 2H), 2.4 (d, *J*=6.7, 2H), 1.6 (d, *J*=13.1, 2H), 1.5 (s, 1H), 1.4 (s, 9H), 1.0 (d, *J*=12.9, 2H).

^{13}C NMR (151 MHz, $CDCl_3$) δ = 161.9 (dd, *J*=588.5, 12.0), 160.2 (dd, *J*=580.7, 12.0), 154.9, 151.6, 145.0, 130.1 – 129.7 (m), 125.1 – 124.9 (m), 111.8 (d, *J*=20.6), 104.4 (t, *J*=26.4), 79.6, 73.3 (d, *J*=5.6), 56.1 (d, *J*=4.2), 55.8, 54.6 (d, *J*=3.7), 44.8 – 42.6 (m), 36.2, 30.1, 28.6.

ESI-MS (m/z): $C_{22}H_{31}F_2N_5O_3$ = 452.2 $[M+H]^+$, **Yield 86% , Rf 0,48 (DCM/MeOH 6%)**

Compound 2b

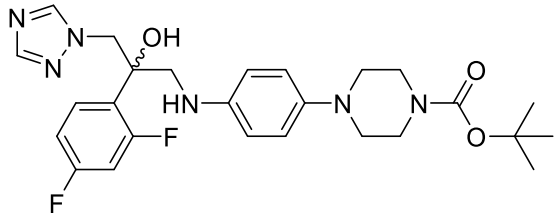

^{1}H NMR (600 MHz, DMSO) δ = 8.3 (s, 1H), 7.7 (s, 1H), 7.4 (q, *J*=7.7, 1H), 7.1 (t, *J*=7.7, 1H), 6.9 (td, *J*=8.5, 2.5, 1H), 6.7 (d, *J*=8.2, 2H), 6.5 (d, *J*=8.2, 2H), 6.0 (s, 1H), 4.9 (s, 1H), 4.7 (d, *J*=14.2, 1H), 4.6 (d, *J*=14.2, 1H), 3.5 – 3.5 (m, 1H), 3.4 – 3.4 (m, 5H), 2.8 (s, 4H), 1.4 (s, 9H).

^{13}C NMR (151 MHz, DMSO) δ = 161.2 (dd, *J*=402.0, 12.3), 159.6 (dd, *J*=403.5, 12.3), 153.8, 150.5, 144.9, 143.3, 142.7, 130.4 – 130.0 (m), 125.3 (d, *J*=12.9), 118.5, 110.8 (d, *J*=20.9), 104.9 – 102.3 (m), 78.9, 74.8 (d, *J*=4.5), 55.2 (d, *J*=3.9), 51.2, 50.5, 44.4 – 42.4 (m), 40.1, 28.1.

ESI-MS (m/z): Found mass for $C_{26}H_{32}F_2N_6O_3$ = 515.2 $[M+H]^+$, **Yield 44%, Rf 0,51 (DCM:MeOH 6%)**

General method of synthesis 3a-b:

To a solution of **2a-b** in DCM (10 mL) was added 3 mL of TFA and the solution stirred for 3 h at 25 °C. The reaction was diluted with 5 mL of PhMe and then concentrated in vacuo. The residue obtained was suspended in ether (10 mL) and sonicated for 5 min. The ether was decanted and the solid formed was dried under vacuum for 1 h.

Compound 3a

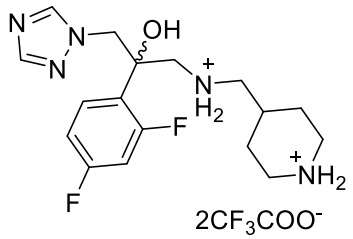

^{1}H NMR (600 MHz, DMSO) δ = 8.8 – 8.7 (m, 1H), 8.6 – 8.5 (m, 1H), 8.5 – 8.4 (m, 2H), 8.3 (s, 1H), 7.8 (s, 1H), 7.5 – 7.4 (m, 1H), 7.3 – 7.2 (m, 1H), 7.1 – 7.0 (m, 1H), 4.7 – 4.6 (m, 2H), 3.6 – 3.5 (m, 1H), 3.4 – 3.3 (m, 1H), 3.3 (d, *J*=13.2, 2H), 2.9 – 2.8 (m, 4H), 2.0 – 1.9 (m, 1H), 1.8 (d, *J*=17.1, 2H), 1.4 – 1.3 (m, 2H).

^{13}C NMR (151 MHz, DMSO) δ = 161.7 (dd, *J*=498.5, 12.1), 160.1 (dd, *J*=497.7, 12.0), 151.0, 145.3, 130.3, 122.6 (d, *J*=13.1), 111.4 (d, *J*=20.3), 104.5 (t, *J*=26.6), 72.1 (d, *J*=4.4), 54.9, 52.3, 42.5, 40.1, 29.8, 26.0 (d, *J*=6.1).

Yield 84%

Compound 3b

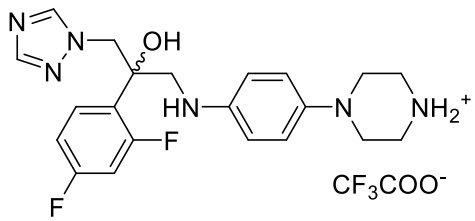

^{1}H NMR (600 MHz, DMSO) δ = 8.8 (s, 2H), 8.3 (s, 1H), 7.8 (s, 1H), 7.5 – 7.3 (m, 1H), 7.2 – 7.1 (m, 1H), 7.0 – 6.9 (m, 1H), 6.8 (d, *J*=8.3, 2H), 6.6 (d, *J*=8.3, 2H), 4.7 – 4.6 (m, 2H), 3.5 (d, *J*=13.3, 1H), 3.4 (d, *J*=13.3, 1H), 3.2 (s, 4H), 3.2 – 3.1 (m, 4H).

^{13}C NMR (151 MHz, DMSO) δ = 161.2 (dd, *J*=410.5, 12.1), 160.1 (dd, *J*=409.5, 12.9), 150.5, 144.9, 143.0, 141.9, 130.3, 125.1, 118.4, 114.0, 110.8 (d, *J*=20.2), 104.4 – 103.0 (m), 74.7, 55.2, 51.4, 47.4, 43.0.

ESI-MS (m/z): Found mass for $C_{21}H_{25}F_2N_6O$= 415.1 $[M]^+$, **Yield 61%**

General method of synthesis 4a-b:

The mixture of hydrochloride 2-(2,4-difluorophenyl)-1-(piperazin-1-yl)-3-(1H-1,2,4-triazol-1-yl)propan-2-ol (mg, 1 eq.), triethylamine (2 eq.) and **2a-2c** (, 1 eq.) stirred in dry DCM overnight. After this, DCM was evaporated, the precipitate dissolved in methylene chloride and washed firstly with aqueous citric acid up to the acidic pH, and then with water. The organic phase was washed saturated sodium chloride solution, then dried over anhydrous Na_2SO_4, filtered, and concentrated in vacuum. The residue was dissolved in methylene chloride and the substance was purified by flash chromatography on silica gel (Hex/EtOAc = 1/4).

Compound 4b

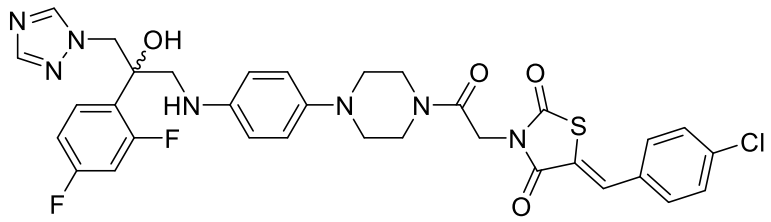

ESI-MS (m/z): Found mass for $C_{33}H_{30}ClF_2N_7O_4S$= 693.3 $[M]^+$, 694.3 $[M+H]^+$, **Yield 59%**

General method of synthesis 5a-b:

To a solution of **1a-c** (mg, mmol) in 5 mL of methanol and 0.2 mL of acetic acid was added formaldehyde (30% weight solution, mL, mmol) under argon at room temperature. Then sodium cyanoborohydride (mg, mmol) was added and the solution was stirred for 24 h. Mixture was diluted with water and the product was extracted with dichloromethane 3×15 ml. Organic layers were combined, was washed saturated sodium chloride and solution dried over anhydrous Na_2SO_4 and concentrated in vacuo. The residue was purified by silica gel column chromatography (dichloromethane : methanol, 25:1).

Compound 5a

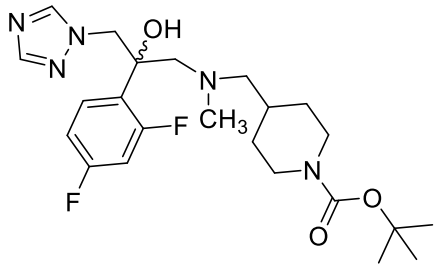

^{1}H NMR (600 MHz, $CDCl_3$) δ = 8.1 (s, 1H), 7.7 (s, 1H), 7.5 (d, *J*=8.8, 1H), 6.8 – 6.6 (m, 2H), 4.5 (d, *J*=14.3, 1H), 4.4 (d, *J*=14.3, 1H), 4.1 – 3.9 (m, 2H), 3.0 (d, *J*=13.5, 1H), 2.7 (d, *J*=13.5, 1H), 2.6 – 2.5 (m, 2H), 2.2 – 2.1 (m, 1H), 2.1 – 2.0 (m, 1H), 2.0 (s, 3H), 1.5 (d, *J*=13.3, 1H), 1.5 (d, *J*=13.2, 1H), 1.4 (s, 9H), 1.3 – 1.3 (m, 1H), 0.9 – 0.8 (m, 2H).

^{13}C NMR (151 MHz, $CDCl_3$) δ = 161.6 (dd, *J*=576.3, 11.8), 160.0 (dd, *J*=573.3, 11.9), 154.8, 150.9, 144.8, 129.6 (dd, *J*=9.4, 5.8), 127.1 – 125.5 (m), 111.5 (d, *J*=20.5), 104.3 (t, *J*=26.3), 79.4, 71.9 (d, *J*=5.5), 65.3, 62.7, 56.4 (d, *J*=4.9), 44.0, 43.6 – 42.7 (m), 34.2, 30.3, 28.4.

ESI-MS (m/z): Found mass for $C_{23}H_{33}F_2N_5O_3$ = 466.3 $[M+H]^+$, **Yield 62%**

The general method of synthesis 6a-b is similar to the synthesis of compounds 4a-b:

Compound 6a

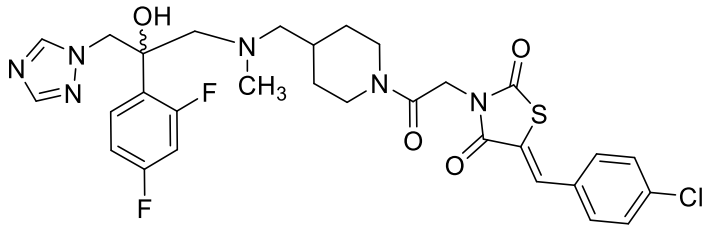

ESI-MS (m/z): Found mass for $C_{34}H_{32}ClF_2N_7O_4S$ = 708.2 $[M+H]^+$

Compound 6b

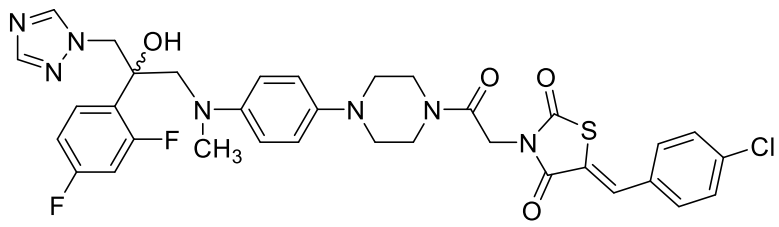

ESI-MS (m/z): Found mass for $C_{30}H_{31}ClF_2N_6O_4S$ = 645.2 $[M+H]^+$

General method of synthesis 7-8:

To a mixture of **2b** (1 mmol) in dry DCM (3 mL) was slowly added TEA (4 mmol) at 0 °C and the solution was stirred for 10 min. Then acetyl chloride (1.2 mmol) was added dropwise to the reaction mixture at 0 °C and it was stirred at room temperature overnight. After the reaction mixture was quenched with sat. NaHCO3 solution and aqueous layer was extracted with EtOAc (3 X 15 mL). The combined organic layer was washed with brine, dried over anhydrous Na_2SO_4 and concentrated in vacuo. The residue was purified by silica gel column chromatography (Hex:EtOAc, 1:4).

Compound 7

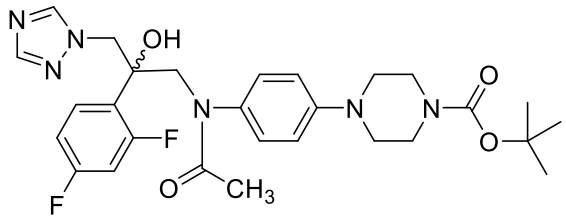

^{1}H NMR (600 MHz, DMSO) δ = 8.3 (s, 1H), 7.7 (s, 1H), 7.4 (t, *J*=8.9, 1H), 7.0 – 6.9 (m, 2H), 6.8 – 6.6 (m, 4H), 6.4 (s, 1H), 4.5 (dd, *J*=21.1, 14.1, 2H), 4.4 (d, *J*=14.4, 1H), 3.9 (d, *J*=14.4, 1H), 3.5 – 3.4 (m, 4H), 3.1 – 3.0 (m, 4H), 1.7 (s, 3H), 1.4 (s, 9H).

^{13}C NMR (151 MHz, DMSO) δ = 173.2, 161.2 (dd, *J*=473.7, 12.7), 159.6 (dd, *J*=474.1, 12.5), 153.9, 150.5, 149.6, 145.1, 135.1, 130.1, 127.9, 124.6 (d, *J*=12.1), 115.7, 110.8 (d, *J*=20.4), 103.6 (t, *J*=27.1), 79.0, 75.3 (d, *J*=5.0), 56.4, 55.5, 48.3 (d, *J*=96.9), 43.8 – 42.3 (m), 28.1, 22.4.

Compound 8

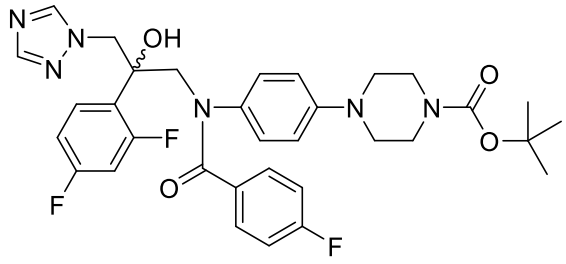

^{1}H NMR (600 MHz, $CDCl_3$) δ = 8.3 (s, 1H), 7.8 (s, 1H), 7.7 (td, *J*=8.8, 6.5, 1H), 7.2 – 7.1 (m, 2H), 7.0 (s, 1H), 6.9 – 6.7 (m, 3H), 6.7 – 6.4 (m, 2H), 6.4 – 6.2 (m, 1H), 4.7 (d, *J*=14.1, 1H), 4.5 – 4.3 (m, 3H), 3.6 – 3.5 (m, 4H), 3.1 – 3.0 (m, 4H), 1.5 (s, 9H).

^{13}C NMR (151 MHz, $CDCl_3$) δ = 172.9, 163.7 (d, *J*=252.2), 161.8 (dd, *J*=617.5, 12.0), 160.2 (dd, *J*=614.9, 12.1), 154.7, 151.1, 149.3, 145.1, 135.5, 131.7 (d, *J*=8.8), 130.8 – 130.3 (m), 130.1 (d, *J*=3.3), 127.7, 124.0 (d, *J*=11.1), 116.5, 115.1 (d, *J*=21.9), 111.5 (d, *J*=20.5), 103.7 (t, *J*=26.5), 80.3, 76.1 (d, *J*=4.6), 58.4 (d, *J*=3.6), 57.0 (d, *J*=5.1), 49.2, 44.8 – 42.3 (m), 28.5.

ESI-MS (m/z): Found mass for $C_{33}H_{35}F_3N_6O_4$ = 637.1 $[M+H]^+$

The general method of synthesis 9-10 is similar to the synthesis of compounds 4a-b:

Compound 9

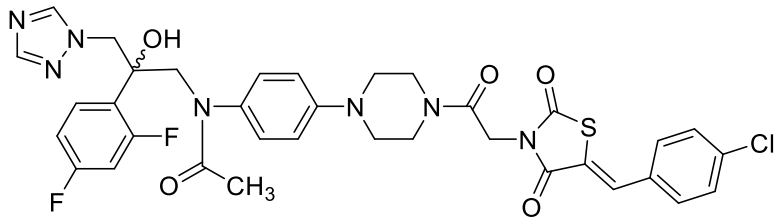

ESI-MS (m/z): Found mass for $C_{35}H_{32}ClF_2N_7O_5S$ = 736.2 $[M+H]^+$

Compound 10

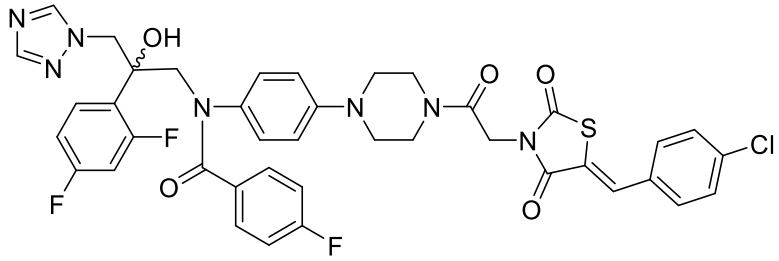

ESI-MS (m/z): Found mass for $C_{40}H_{33}ClF_3N_7O_5S$ = 816.3 $[M+H]^+$

【評語】030030

This study emphasizes the potential of hybrid triazole-TZD molecules in overcoming resistance and enhancing antifungal efficacy. The results confirm the feasibility of synthesizing piperazine derivatives containing both triazole and thiazolidine fragments using various linkers. Drug resistance remains a significant challenge in pharmaceutical synthesis, and addressing it requires substantial effort in research. Overall, this is a commendable and well-executed piece of work.